Rigorous Analysis of Probe-Fed Printed Annular Ring Antennas

David M. Kokotoff, James T. Aberle, and Rod B. Waterhouse, *Member, IEEE*

***Abstract*—This paper presents calculated and measured results for the input impedance and radiation performance of probe-fed printed annular ring antennas. Geometries featuring stacked rings as well as shorting posts are considered. A numerical model is presented that is based on a full-wave spectral-domain moment-method solution. In this solution, a specialized attachment mode-expansion function is used to model the connection between the probe feed and the printed ring. Measured results are presented and compare well with the theory. Annular rings are found to have certain advantages over circular and rectangular microstrip antennas.**

***Index Terms*—Microstrip antennas.**

I. Introduction

MICROSTRIP patch antennas are used in a variety of applications due to their many salient features [1]. Like many forms of microstrip patches, the annular ring has received considerable attention. When operated in its fundamental mode, TM_{11}, this printed antenna is smaller than its rectangular or circular counterparts. The annular ring may also be somewhat broadband in nature when operated near the TM_{12} resonance [2]. For these reasons, there have been several theoretical and experimental investigations into the performance of printed annular rings [2]–[4]. Feeding a printed antenna via a coaxial probe has long been established as the most robust means of coupling power to and from a microstrip patch. This coupling technique also provides excellent isolation between the components of the feeding network (e.g., phase shifters and amplifiers) and the radiating elements, reducing the likelihood of spurious coupling as well as unwanted back radiation. Such requirements are critical when developing arrays positioned back to back as in typical mobile communication base station environments.

To accurately model a microstrip patch antenna fed by a coaxial probe, special consideration of the current discontinuity associated with the probe and patch conductors must be made [5]. Approximate models, such as the cavity model, although they give good insight into some of the general trends of the antenna, fail to give an accurate representation of the performance, especially when an electrically thick (say, greater than $0.02\lambda_o$) substrate is used. Such conditions are encountered when attempting to enhance the bandwidth of a printed antenna to meet commercial system performance requirements. For these situations, a rigorous full-wave analysis must be used.

In this paper, we present a rigorous full-wave spectral domain analysis that can accurately model the performance of a probe-fed annular ring. Central to this analysis is a specially derived attachment mode that accurately models the current on the probe feed and also the discontinuity between the feed and ring conductors. An overview of the derivation of the attachment mode is given. Furthermore, some design examples using the derived analysis, namely, stacked and shorted annular rings are given. Some pertinent advantages of utilizing printed annular rings for these patch antenna configurations are also discussed.

II. Theory

Consider a stacked annular probe-fed microstrip patch antenna on an infinite grounded dielectric slab with dimensions shown in Fig. 1. The printed element, the probe feeds, and the ground plane are all assumed to be perfect conductors. The feed region is modeled as a delta-gap voltage generator between the base of the probe and ground plane.

The formulation is a full-wave spectral-domain moment-method approach [5] and, for the sake of brevity, will not be discussed. As in [5], the unknown electric current density on the patches are approximated by a set of vector expansion functions with unknown coefficients. These expansion functions are based on the eigenmodes of the magnetic wall cavity model of an annular ring geometry [6]. Additionally, each probe has a special entire domain expansion function, $\bar{f}_i^a$, associated with it. This expansion function is commonly referred to as an attachment mode.

The annular ring attachment mode implemented here is an application of the concept originally proposed by Aberle [5], [7], [8] for a circular-patch geometry. In this approach, an attachment mode appropriate to the geometry under consideration is derived from the corresponding cavity model, assuming a uniform filamentary source. This expansion function properly models the underlying physics of the problem and, hence, greatly enhances the accuracy and efficiency of the solution.

For an annular ring patch, the patch part of the attachment mode in the spatial domain can be written

$$f_x^a(\rho,\phi) = f_\rho(\rho,\phi)\cos\phi - f_\phi(\rho,\phi)\sin\phi \quad (1)$$

$$f_y^a(\rho,\phi) = f_\rho(\rho,\phi)\sin\phi + f_\phi(\rho,\phi)\cos\phi \quad (2)$$

Manuscript received March 27, 1998; revised June 15, 1998.

D. M. Kokotoff and R. B. Waterhouse are with the Department of Communication and Electronic Engineering, Royal Melbourne Institute of Technology, Melbourne, VIC 3001, Australia.

J. T. Aberle is on sabbatical from the Royal Melbourne Institute of Technology. He is now with the Telecommunications Research Center, Arizona State University, Tempe, AZ 85287 USA.

Publisher Item Identifier S 0018-926X(99)03717-5.

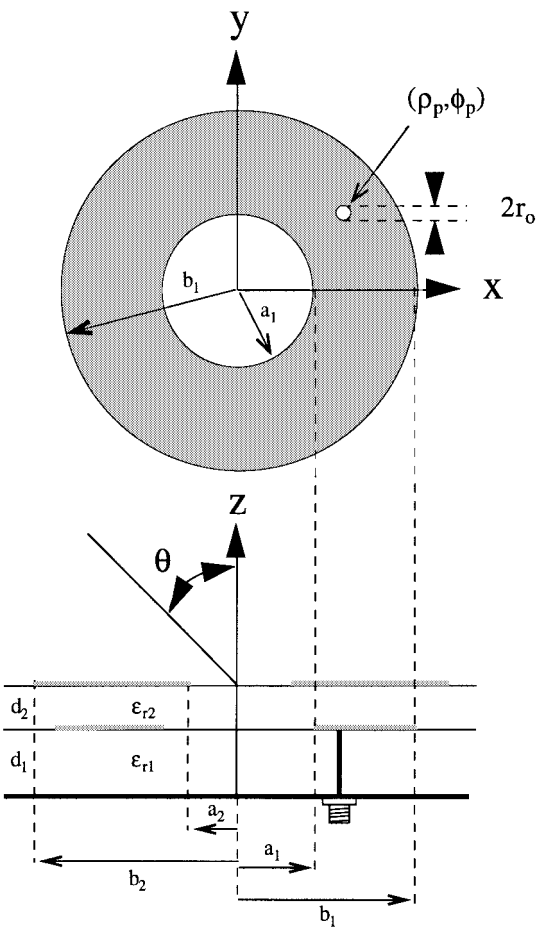

Fig. 1. Geometry of a stacked probe-fed printed annular ring with appropriate symbols.

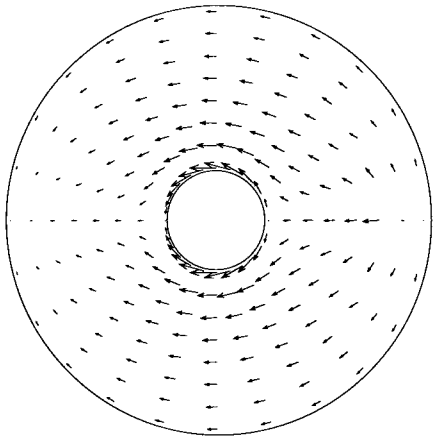

(a)

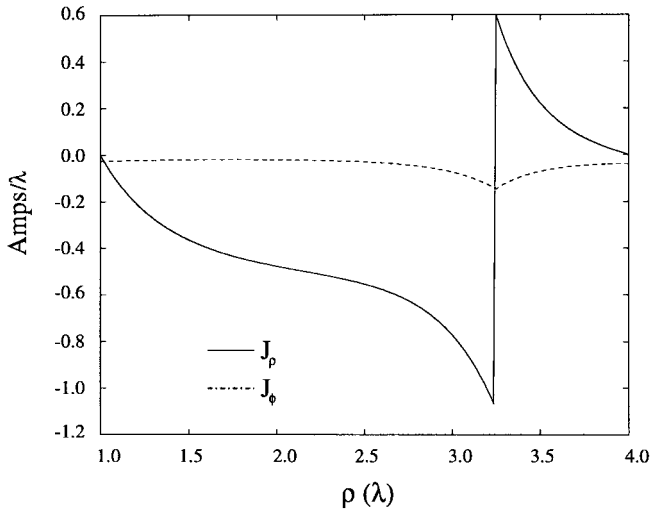

(b)

Fig. 2. (a) Vector and (b) linear plot ($\lambda < \rho < 4\lambda$ and $\phi = 0^o$) of the patch part of the attachment mode-expansion function ($k = \frac{0.38}{\lambda}, a_1 = \lambda, b_1 = 4\lambda, \rho_p = 3.25\lambda, \phi_p = 1^o$).

where f_ρ and f_ϕ are given by a series of ordinary Bessel functions,

$$f_\rho(\rho,\phi) = -\frac{k}{4}\sum_{m=0}^{\infty}\epsilon_m\cos(m(\phi-\phi_p)) \times \begin{cases} A_m[Y'_m(ka)J'_m(k\rho)-J'_m(ka)Y'_m(k\rho)] & \rho\le\rho_p \\ B_m[Y'_m(kb)J'_m(k\rho)-J'_m(kb)Y'_m(k\rho)] & \rho\ge\rho_p \end{cases} \tag{3}$$

$$f_\phi(\rho,\phi) = \frac{1}{2\rho}\sum_{m=1}^{\infty} m\sin(m(\phi-\phi_p)) \times \begin{cases} A_m[Y'_m(ka)J_m(k\rho)-J'_m(ka)Y_m(k\rho)] & \rho\le\rho_p \\ B_m[Y'_m(kb)J_m(k\rho)-J'_m(kb)Y_m(k\rho)] & \rho\ge\rho_p \end{cases} \tag{4}$$

k is the wavenumber in the material, ρ_p and ϕ_p are the probe position in cylindrical coordinates, ϵ_m is Neumann number [5], and the coefficients A_m and B_m are given by

$$A_m = \frac{Y'_m(kb)J_m(k\rho_p)-J'_m(kb)Y_m(k\rho_p)}{Y'_m(ka)J'_m(kb)-J'_m(ka)Y'_m(kb)} \tag{5}$$

$$B_m = \frac{Y'_m(ka)J_m(k\rho_p)-J'_m(ka)Y_m(k\rho_p)}{Y'_m(ka)J'_m(kb)-J'_m(ka)Y'_m(kb)}. \tag{6}$$

Fig. 2 plots the patch part of the attachment mode in both vector and linear form. As seen in the linear plot, in the vicinity of the probe location, the attachment mode becomes singular. However, the mode is well behaved over the remainder of the structure as shown in the vector plot. The negative current in Fig. 2(b) represents a change in the vector direction of the current. For this case, the current resembles the dominant TM_{11} mode of the patch. Hence, the attachment mode is a good approximation to the original problem.

In the spectral-domain technique, the Fourier transform of the basis set is necessary. By the use of some relatively straightforward, albeit tedious, manipulations, the Fourier transform, denoted by the superscript "$\sim$" of the patch portion of the attachment mode can be evaluated in polar spectral form. The final form of the attachment mode transform is

$$\tilde{f}_x = -\jmath\{T_1(\beta,\alpha)\cos\alpha + T_2(\beta,\alpha)\sin\alpha\} \tag{7}$$

$$\tilde{f}_y = -\jmath\{T_1(\beta,\alpha)\sin\alpha - T_2(\beta,\alpha)\cos\alpha\} \tag{8}$$

with T_1 and T_2 given by

$$T_1(\beta,\alpha) = \frac{kS_1(\beta,\alpha) - \beta S_2(\beta,\alpha)}{k^2 - \beta^2} \tag{9}$$

$$T_2(\beta,\alpha) = \frac{S_3(\beta,\alpha)}{k\beta b} \tag{10}$$

and

$$S_1(\beta,\alpha) = \sum_{m=0}^{\infty} \epsilon_m \jmath^{-m} \cos(m(\alpha-\phi_p)) \times [A_m J'_m(\beta b) - B_m J'_m(\beta a)] \tag{11}$$

$$S_2(\beta,\alpha) = e^{-\jmath\beta\rho_p\cos(\alpha-\phi_p)} \tag{12}$$

$$S_3(\beta,\alpha) = 2\sum_{m=1}^{\infty} m\jmath^{-m}\sin(m(\alpha-\phi_p)) \times \left[A_m J_m(\beta b) - \frac{b}{a} B_m J_m(\beta a)\right]. \tag{13}$$

The polar spectral coordinates β and α are related to the Cartesian spectral coordinates k_x and k_y, as given in [5]. It is interesting to note that the form of the Fourier transform is quite similar to that of the circular patch attachment mode [5], with only A_m and B_m differing.

The expansion set can now be substituted into the operator equation (see [5] for details) and can be tested to reduce the problem to a matrix equation. Due to the inherent ϕ-symmetry of the structure, the two-dimensional spectral integration associated with each matrix element can be reduced to a single semi-infinite integration with respect to β. This yields a large computational savings as compared to the rectangular probe-fed patch. The derivation and evaluation of the individual matrix elements follows [8].

Note, that for the purposes of testing the operator equation, the part of the testing functions which exist on the probe feed is not assumed to be filamentary, but includes the radius of the probe [5], [7], [8]. This adds to the accuracy of the method, since the radius of the probe is considered; however, it removes the symmetry of the attachment mode portion of the system matrix.

Once the matrix equation is solved for the unknown coefficients, the input impedance, radiated field and other electrical signatures can be evaluated using an analogous procedure to [8].

III. Results

A. Stacked Annular Ring

The impedance variation of a single-layer printed annular ring has been thoroughly examined in the literature both experimentally and theoretically [2], [3]. For this reason and for the sake of brevity, an investigation is not included here. There are, however, several features of a probe-fed printed annular ring which are pertinent to the more complicated design examples presented here. In particular, when operating in the fundamental mode (TM_{11}) the probe-fed printed ring has a high-input impedance at resonance [2]. Thus, there is a strong coupling between the feed and the patch; that is, the radiator is overcoupled. This is why proximity coupling a microstrip line to a printed ring is the preferred option. Hence, by moving the feedline away from the patch, the coupling to the radiator and the input impedance can be reduced [9]. However, the strong coupling between a probe feed and a printed annular ring is extremely advantageous when considering stacked configurations. Typically for any stacked patch configuration, the lower resonator is deliberately overcoupled and the top patch is used to effectively impedance match the entire configuration. Thus, the high impedance encountered for a probe-fed single layered ring is well suited to a stacked version. Importantly too, the high impedance level is relatively independent of substrate thickness. Thus, thick dielectric layers below the lower resonator can be used without the penalty of poorly behaved input impedance due to the inductive nature of the feed. This is in direct contrast to probe-fed circular and rectangular stacked patch configurations where the lower substrate cannot be made too thick. Another advantage of the annular ring over the circular patch version is the extra degree of freedom in design, namely the inner radius. This may be varied independently of the outer radius to provide fine tuning of the impedance variation of the antenna. The effect of this extra degree of freedom is similar to varying the width of a rectangular patch.

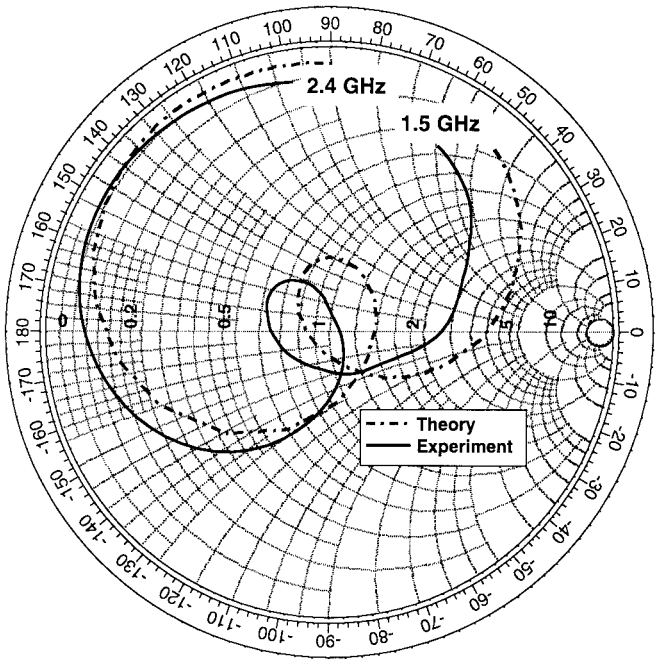

Fig. 3. Predicted and measured input impedance of the stacked probe-fed stacked annular ring ($\epsilon_{r1} = 2.2$, $\tan\delta_1 = 0.001$, $d_1 = 6.096$ mm, $a_1 = 10.0$ mm, $b_1 = 29.0$ mm, $\rho_p = 21.0$ mm, $\phi_p = 0^o$, $r_o = 0.325$ mm, $\epsilon_{r2} = 1.07$, $\tan\delta_2 = 0.001$, $d_2 = 8.0$ mm, $a_2 = 14.0$ mm, $b_2 = 31.0$ mm).

Fig. 3 shows the predicted and measured input impedance plot of a probe-fed stacked annular ring antenna (refer to the caption for the relevant dimensions). As can be seen from Fig. 3, very good agreement between theory and experiment is achieved. The predicted and measured 10-dB return loss bandwidth is 21% and 22%, respectively. The variation between the experimental and theoretical impedance loci is due to the positional error in the alignment of the top patch and the thin layer of dielectric material required to etch this

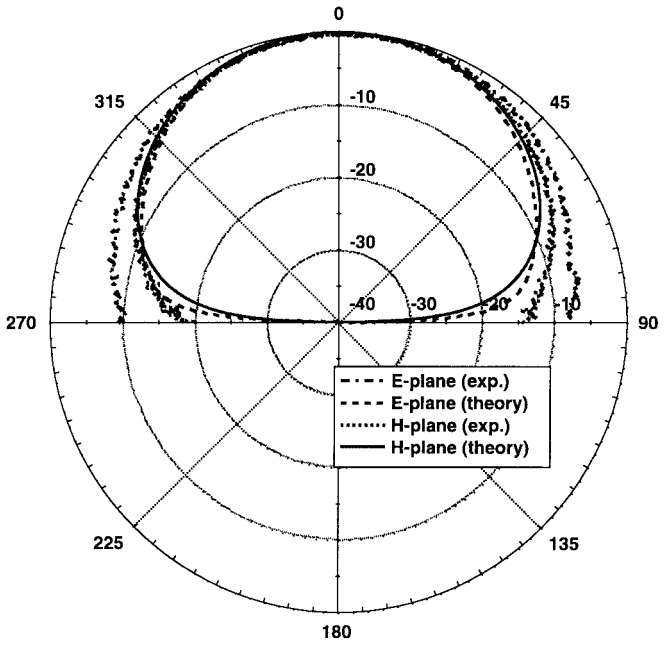

Fig. 4. Measured and calculated E- and H-plane co-polar radiation patterns for the stacked annular ring (refer to Fig. 3's caption for parameters).

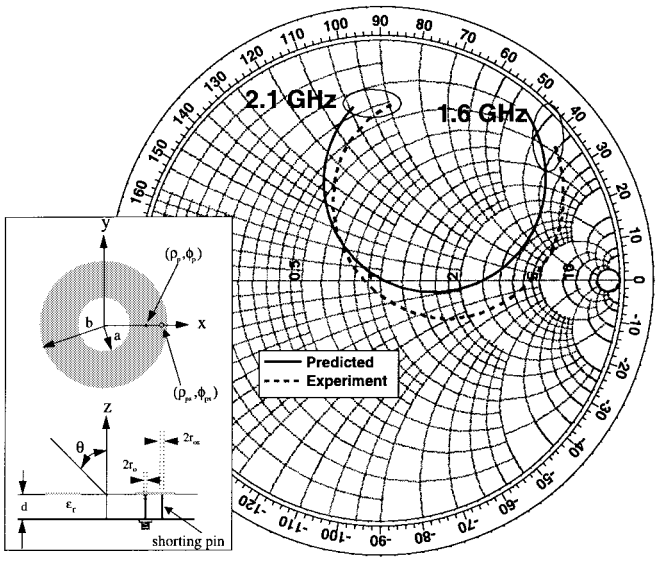

Fig. 5. Measured and calculated input impedance behavior (and schematic) of a shorted probe-fed printed annular ring ($\epsilon_r = 1.07$, $\tan\delta = 0.001$, $d = 10.0$ mm, $a = 6.0$ mm, $b = 10.3$ mm, $\rho_p = 7.0$ mm, $\phi_p = 0^o$, $r_o = 0.325$ mm, $\rho_{ps} = 9.3$ mm, $\phi_{ps} = 0^o$, $r_{os} = 0.6$ mm).

conductor. This layer (thickness $= 0.254$ mm, $\epsilon_r = 2.2$) is not included in the analysis. The central processing unit (CPU) time per frequency point using 15 entire domain expansion functions on each patch and the attachment mode is 18 s using a 200 MHz AMD K6 running LINUX. The E- and H-plane co-polar and cross-polar far-field radiation patterns were measured and are very similar to a conventional patch radiation characteristics. Comparisons of these measured values and the predicted results for the E-plane and H-plane co-polar patterns are shown in Fig. 4. Both the measured and predicted cross-polarization levels are greater than 20 dB below the peak values in both planes. The gain of the stacked configuration is measured as 8.2 dBi, compared to a theoretical value of 8.5 dBi.

B. Shorted Annular Ring

Patches incorporating a single shorting post strongly coupled to the feeding mechanism have been shown to be significantly smaller than conventional and even quarter-wave patches [10]–[13]. These small printed antennas have been proposed for applications such as mobile communication handset terminals. The single shorting post design strategy can also be applied to a printed annular ring to further reduce its surface area. Importantly, as shown in [10] and [11], to accurately analyze such a printed antenna, attachment modes are required to account for the current discontinuities between the pins and the patch conductor as well as the coupling between the shorting post and the feed.

Fig. 5 shows a schematic of a shorted annular ring and the input impedance variation of such an antenna using 10-mm 51 HF Rohacell foam as the substrate. The dimensions of the structure are given in the figure caption. As seen from the measured and predicted impedance loci, very good agreement is evident. The predicted and measured 10-dB return loss bandwidths of the antenna are 5.8% and 5.9%, respectively. The slight shift in resonant frequency apparent in Fig. 5 can be attributed to the thin layer of dielectric material required to etch the patch conductor. Again, this layer is not included in the analysis. For the theoretical results displayed in Fig. 5, two attachment modes and 25 entire-domain basis functions were used. The impedance bandwidth achieved here is suitable for most digital cordless systems [14]. The radiation patterns of the shorted ring were measured and are very similar to those presented in [11] for a shorted circular patch. For the sake of brevity these patterns will not be given here. The gain of the antenna is measured as 3.5 dBi compared to a theoretical value of 3.6 dBi.

It is interesting to compare the properties of the shorted annular ring with previously presented shorted patches [11]. Using the same dielectric materials, the outer radius of the shorted ring is slightly smaller than the radius of a circular shorted patch, by approximately 5%. The bandwidth and the gain of the shorted ring are once again slightly less than the circular patch version by 0.5% and 0.2 dBi, respectively. These results can be attributed to the smaller area of the new antenna. Despite these relative shortcomings in the electrical performance of the shorted annular ring, there is a distinct advantage. The gap between the shorting and feed pins is 14% greater. This allows for easier manufacturing of the antenna and makes it less susceptible to errors in the positioning of these pins [13]. As is shown in [11], the coupling between the feed, the shorting post and the closest radiating edge plays a significant role in the impedance behavior and, hence, the size of the patch. Like the stacked patch case considered earlier, the annular ring has another degree of freedom that contributes to the impedance behavior, namely, the inner radius of the conductor. Thus the strong capacitive coupling required for a shorted patch to operate can be distributed amongst all these variables. It is shown in [11] that for

minimum area the shorting pin must be located closest to one of the radiating edges of the patch. However, it is also shown that for maximum spacing between the feed and shorting pins, the feed should be located nearest to this edge. Hence, for a circular or rectangular patch configuration, a compromise must be made. However, by using an annular ring both criterion may be achieved. Here, the feed pin is located nearest the inner edge and the shorting pin located near the outer edge of the ring. This creates a shorted patch of minimal area as well as acceptable spacing between the pins.

IV. Conclusion

The input impedance and radiation performance of probe-fed annular microstrip antennas has been investigated. A rigorous numerical model based on a full-wave spectral-domain moment-method solution has been used. To properly account for the connection between the probe feed and the patch, a special attachment mode has been derived and used. Besides ensuring the continuity of current at attachment point, this expansion mode also accounts for the singular nature of the current about this point. Due to the inherent ϕ symmetry of the structure, the two-dimensional spectral integration can be reduced to a single integration. This yields a large computational savings as compared to the spectral-domain moment-method solution of rectangular probe-fed patch.

Measured results for both the stacked and shorting post cases are presented and compare well with this theory. In particular, the high-impedance nature of the probe-fed annular ring and the constant impedance versus substrate thickness for the dominant TM_{11} mode is used advantageously in the stacked configurations. Impedance bandwidths in excess of 20% and a gain of over 8 dBi are achieved both theoretically and experimentally. Also, the shorting post version of the annular ring has the advantage of a larger spacing (14%) between the probe and shorting pin with virtually identical electrical performance over 5% impedance bandwidth with a gain of over 3.5 dBi, as compared to its circular patch counterpart. This suggests that the tolerances on the feed probe/shorting post position is loosened in the annular ring case. In either case, the additional degree of freedom of the inner radius of the conductor is similar to the width of a rectangular patch and assists in the design process.

References

[1] D. M. Pozar, "Microstrip antennas," in *Proc. IEEE*, vol. 80, pp. 79–91, Jan. 1992.
[2] W. C. Chew, "A broad-band annular-ring microstrip antenna," *IEEE Trans. Antennas Propagat.*, vol. AP-30, pp. 918–922, May 1982.
[3] J. S. Dahelle and K. F. Lee, "Characteristics of annular ring microstrip antenna," *Electron. Lett.*, vol. 18, pp. 1051–1052, Nov. 1982.
[4] A. K. Bhattacharyya and R. Garg, "Input impedance of annular ring microstrip antenna using circuit theory," *IEEE Trans. Antennas Propagat.*, vol. AP-33, pp. 369–374, Apr. 1985.
[5] J. T. Aberle and D. M. Pozar, "Accurate and versatile solutions for probe-fed microstrip patch antennas and arrays," *Electromagn.*, vol. 11, pp. 1–19, Jan. 1991.
[6] Z. Nie, W. C. Chew, and Y. T. Lo, "Analysis of the annular-ring-loaded circular disk microstrip antenna," *IEEE Trans. Antennas Propagat.*, vol. 38, pp. 806–813, June 1990.
[7] J. T. Aberle, D. M. Pozar, and J. Manges, "Phased arrays of probe-fed stacked microstrip patches," *IEEE Trans. Antennas Propagat.*, vol. 42, pp. 920–927, July 1994.
[8] J. T. Aberle, "Analysis of probe-fed circular microstrip antennas," Ph.D. dissertation, Univ. Massachusetts, Amherst, MA, May 1989.
[9] M.-J. Tsai and N. G. Alexopoulos, "Electromagnetically coupled microstrip ring-type antennas of arbitrary shape," *IEEE Antennas Propagat. Soc. Int. Symp.*, Newport Beach, CA, July 1995, pp. 684–687.
[10] R. B. Waterhouse, "Small microstrip patch antenna," *Electron. Lett.*, vol. 31, pp. 604–605, Apr. 1995.
[11] R. B. Waterhouse, S. D. Targonski, and D. M. Kokotoff, "Design and performance of small printed antennas," *IEEE Trans. Antennas Propagat.*, vol. 46, pp. 1629–1633, Nov. 1998.
[12] I. Park and R. Mittra, "Aperture-coupled small microstrip antenna," *Electron. Lett.*, vol. 32, pp. 1741–1742, Sept. 1996.
[13] R. B. Waterhouse and D. M. Kokotoff, "Novel technique to improve the manufacturing ease of shorted patches," *Microwave Opt. Technol. Lett.*, vol. 17, pp. 37–40, Jan. 1998.
[14] F. Ali and J. B. Horton, "Introduction to special issue on emerging commercial and consumer circuits, systems, and their applications," *IEEE Trans. Microwave Theory Tech.*, vol. 43, pp. 1633–1638, July 1995.

David M. Kokotoff received the B.S.E.E. degree from Lafayette College, Easton, PA, in 1985, the M.S.E.C.E. degree from the University of Massachusetts, Amherst, in 1987, and the Ph.D. degree from Arizona State University, Tempe, in 1995.

From 1987 to 1992, he was employed by Atlantic Aerospace Electronics Corporation, Greenbelt, MD, as a member of the Advanced Antenna Development Group. Since completing his Ph.D., he has been a Lecturer with the Department of Communication and Electronic Engineering, Royal Melbourne Institute of Technology (RMIT) University, Melbourne, Australia. His professional interests focus on applied electromagnetics emphasizing computer-aided design of antennas, microwave, and optical devices.

James T. Aberle received the B.S. and M.S. degrees in electrical engineering from the Polytechnic Institute of New York (now Polytechnic University), Brooklyn, in 1982 and 1985, respectively, and the Ph.D. degree in electrical engineering from the University of Massachusetts, Amherst, in 1989.

From 1982 to 1985, he was with Hazeltine Corporation, Greenlawn, NY, where he worked on the development of wide-band phased array antennas. He was a Graduate Research Assistant at the University of Massachusetts from 1985 to 1989, where he developed and validated computer models for printed antennas. He has been a faculty member at Arizona State University, Tempe, since 1989, where he is currently an Associate Professor of Electrical Engineering. His research interests include the modeling of complex electromagnetic phenomena. He was a NASA/ASEE Summer Faculty Fellow at NASA Langley Research Center during the summer of 1993. During the 1997–1998 academic year, he took a sabbatical leave from Arizona State Universityand was a Visiting Academic at the Royal Melbourne Institute of Technology in Melbourne, Victoria, Australia as well as a Visiting Researcher at Atlantic Aerospace Electronics Corp., Greenbelt, MD.

Rod B. Waterhouse (SM'89–M'94) received the Bachelor of Electrical Engineering (honors), Masters of Engineering Science (research), and the Ph.D. degrees from the University of Queensland, Australia, in 1987, 1990, and 1994, respectively.

In 1994, he joined the Department of Communication and Electronic Engineering at the Royal Melbourne Institute of Technology (RMIT), where he is currently a Senior Lecturer and the Discipline Leader of the Radio Frequency/Photonics Research Group. He has consulted for several companies including Radio Frequency Systems and British Aerospace in the areas of microwave and antenna technology. His research interests include printed antennas, phased arrays, design of antennas suitable for mobile communication systems and optically distributed microwave systems.

Dr. Waterhouse is the Microwave Theory and Technique and Antennas and Propagation chapter chair for the IEEE Victorian Section. In 1999 he was awarded an Australian Research Council (ARC) Grant on fiber feeder networks for LMDS. He has also received ARC funding for projects related to integrated photonic/antenna modules and optical phase shifters.